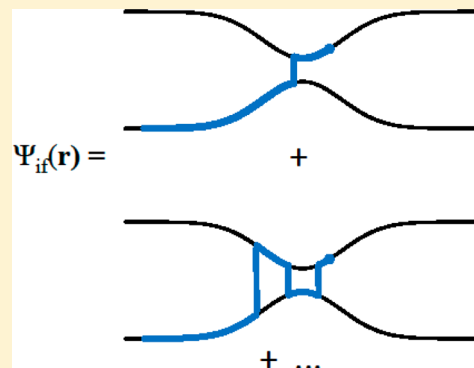


# Improving the Efficiency of Monte Carlo Surface Hopping Calculations

Michael F. Herman

Department of Chemistry, Tulane University, New Orleans, Louisiana 70118, United States

**ABSTRACT:** A surface hopping method with a Monte Carlo procedure for deciding whether to hop at each step along the classical trajectories used in the semiclassical calculation is discussed. It is shown for a simple one-dimensional model problem that the numerical efficiency of the method can be improved by averaging over several copies of the sections of each trajectory that span the interaction regions. The use of Sobol sequences in the selection of the initial momentum for the trajectories is also explored. It is found that accurate results can be obtained with relatively small trajectory samples.



## I. INTRODUCTION

Semiclassical methods provide useful approximations to quantum wave functions, propagators, transition probabilities, and correlation functions. A number of semiclassical approaches have been developed for problems in which nonadiabatic transitions play a significant role.<sup>1–33</sup> These include Erhenfest methods,<sup>3–7</sup> the mapping method,<sup>8–11</sup> and surface hopping methods.<sup>12–33</sup> It has been shown that a particular form of the surface hopping wave function or propagator formally satisfies the Schrodinger equation.<sup>29–33</sup>

This surface hopping method has been found to provide very accurate results for simple one-dimensional model curve crossing problems, even for cases which have significant quantum interference between contributions from hopping during different crossing of the interaction regions.<sup>34–36</sup> If a Monte Carlo procedure is used to decide when to hop to a different adiabatic state as trajectories are evaluated, then the efficiency of the Monte Carlo surface hopping is improved by using “hopping steps” that are much longer than the step size for the numerical integration of the trajectory.<sup>34,35</sup> A hop or not hop decision is made for each hopping step. Wave function amplitudes for staying in the same state and for hopping to a different state are evaluated for the hopping step. The use of longer hopping steps is possible if higher order transition amplitudes for these hopping steps are employed. These higher order transition amplitudes account for the fact that the semiclassical phase factor associated with a given hopping trajectory depends on where the hop or hops occur within this hopping step.<sup>34–36</sup> It was shown in previous calculations on a one-dimensional two-state problem with two crossings of the diabatic state energies that results with an error on the order of 0.01 in the transition probabilities can be achieved in Monte Carlo simulations with 40 000 surface hopping trajectories.<sup>36</sup>

In this work, it is explored, using the same one-dimensional/two-state system, how the number of trajectories goes down if a less strict error tolerance (e.g., 0.03 or 0.05) is deemed acceptable. It is found that the number of trajectories required can be significantly reduced if several copies of the interaction region segments of the trajectory are run. Each of these short segments would have a different Monte Carlo hopping history in the interaction region, and the contribution to the wave function amplitude at the end of the interaction region is obtained by averaging over the contributions from the several trajectory segments.

The use of Sobol sequences to sample the initial momentum for the trajectories is also explored.<sup>37–40</sup> Sobol sequences provide values of  $x$  that uniformly cover the region between 0 and 1 for any number of sampled points. In contrast, if the points are sampled using a random number generator, the set of points is much less uniform. As a result, the error in the integration over the initial momentum distribution decreases more rapidly with increasing sample size using Sobol sequences. On the other hand, a random number generator is employed when making the decision to hop or not during each hopping step of every trajectory in all calculations. Thus, it is of interest to see to what extent the use of Sobol sequences in sampling the initial momentum provides better statistics in the surface hopping calculations.

The form used for state-to-state probabilities,  $P_{ij}(t)$ , in the surface hopping calculations is derived in section II. The diabatic energy surfaces that define the two-state model are presented in section III. In addition, the calculational method is

**Special Issue:** James L. Skinner Festschrift

**Received:** January 31, 2014

**Revised:** March 17, 2014

described in detail and formulas for the higher order amplitudes for the hopping steps are provided. Results for calculations with different values of  $N$  and  $n$  are presented, where  $N$  is the number of trajectory pairs in a calculation and  $n$  is the number of trajectory segments across each interaction region for a given trajectory. The results are summarized, and modifications in the form of  $P_{ij}(t)$  that could be used when performing multi-dimensional calculations are discussed in section IV.

## II. THEORY

The semiclassical (SC) surface hopping propagator can be expressed as<sup>30–33</sup>

$$\mathbf{K}(\mathbf{x}_0, \mathbf{x}, t) = \mathbf{K}^{(0)}(\mathbf{x}_0, \mathbf{x}, t) + \mathbf{K}^{(1)}(\mathbf{x}_0, \mathbf{x}, t) + \mathbf{K}^{(2)}(\mathbf{x}_0, \mathbf{x}, t) \dots \quad (1)$$

where  $K_{ij}^{(0)}(\mathbf{x}_0, \mathbf{x}, t) = \langle \varphi_i | \mathbf{K}^{(0)}(\mathbf{x}_0, \mathbf{x}, t) | \varphi_j \rangle = \delta_{ij} A \exp(iS_i/\hbar)$  is  $\delta_{ij}$  multiplied by the single state semiclassical propagator<sup>41,42</sup> with the system in the  $i$ th Born–Oppenheimer (BO) electronic state  $\varphi_i$  and  $\langle \dots \rangle$  indicates integration over the electronic coordinates. The action  $S_i = \int_0^t L dt_1 - n_c \pi/2$  is evaluated over the trajectory that goes from  $\mathbf{x}_0$  to  $\mathbf{x}$  in time  $t$  with the system in state  $\varphi_i$ , where  $L$  is the Lagrangian and  $n_c$  is the number of caustics encountered along the trajectory. The prefactor has the form  $A = [(-2\pi i \hbar)^{-d} \|\partial^2 S_i / \partial \mathbf{x}_0 \partial \mathbf{x}\|]^{1/2}$ , and  $\|\partial^2 S_i / \partial \mathbf{x}_0 \partial \mathbf{x}\|$  is the absolute value of the determinant  $|\partial^2 S_i / \partial \mathbf{x}_0 \partial \mathbf{x}|$ .  $K_{ij}^{(n)}(\mathbf{x}_0, \mathbf{x}, t) = \langle \varphi_i | \mathbf{K}^{(n)}(\mathbf{x}_0, \mathbf{x}, t) | \varphi_j \rangle$  is the contribution to the propagator from trajectories with  $n$  hops starting at  $\mathbf{x}_0$  in state  $\varphi_i$  and ending at  $\mathbf{x}$  in state  $\varphi_j$ . For instance,  $K_{ij}^{(2)}(\mathbf{x}_0, \mathbf{x}, t)$  has the form

$$K_{ij}^{(2)}(\mathbf{x}_0, \mathbf{x}, t) = \sum_j \int d\mathbf{r}_2 \int d\mathbf{r}_1 \cdot \boldsymbol{\tau}_{ij} \cdot \boldsymbol{\tau}_{jf} A e^{iS/\hbar} \quad (2)$$

where  $S$  is the action for the trajectory that starts in state  $\varphi_i$ , hops to state  $\varphi_j$  at the point  $\mathbf{r}_1$  along the trajectory, hops to state  $\varphi_f$  at the point  $\mathbf{r}_2$ , and then continues in this state to the final point  $\mathbf{x}$  in time  $t$ . The vector amplitude,  $\boldsymbol{\tau}_{jk}$ , for the hop from adiabatic energy surface  $U_j$  to  $U_k$  is defined as

$$\boldsymbol{\tau}_{jk} = -\frac{(p_{j\parallel} + p_{k\parallel})}{2\sqrt{p_{j\parallel}p_{k\parallel}}} \boldsymbol{\eta}_{jk} \quad (3)$$

where  $\boldsymbol{\eta}_{jk}$  is the nonadiabatic coupling vector and  $p_{j\parallel}$  ( $p_{k\parallel}$ ) is the magnitude of the component of the momentum in the  $\boldsymbol{\eta}_{jk}$  direction just before (after) the hop. In eq 2,  $d\mathbf{r}_1$  is dotted into  $\boldsymbol{\tau}_{ij}$  and  $d\mathbf{r}_2$  is dotted into  $\boldsymbol{\tau}_{jf}$ . The component of the momentum in the direction of  $\boldsymbol{\eta}_{ik}$  is altered at each hopping point so that energy is conserved along the trajectory.  $A$  is defined as above using the derivatives of the action for the hopping trajectory,  $S$ . The  $K_{ij}^{(n)}(\mathbf{x}_0, \mathbf{x}, t)$  is similar, except that it has  $n$   $\boldsymbol{\tau}_{ij}$  factors and  $n$  integrations over the hopping points corresponding to the  $n$  hops along the trajectory.

If the trajectory is broken into small steps, as is done in numerical calculations, then the entire surface hopping expansion can be written as

$$K_{ij}(\mathbf{x}_0, \mathbf{x}, t) = \sum_a \prod_m B_{am}^{(m)} A \quad (4)$$

where  $B_{jk}^{(m)} = b_{jk} \exp(iS_{jk}/\hbar)$  is the complex amplitude for the  $m$ th step, given the system is in the  $j$ th BO state at the beginning of the step and in the  $k$ th BO state at the end of the step. In calculations, these amplitudes are evaluated over “hopping steps” that are typically longer than the step size used

in the numerical evaluation of the trajectories. (In the following, step will always refer to hopping steps.) The summation in eq 4 is over every possible sequence of hops and nonhops for the steps in a trajectory, with the condition that the system is in state  $\varphi_i$  at the beginning of the trajectory and in state  $\varphi_f$  at the end of the trajectory. Since it is not, in general, feasible to sum every term in eq 4, a Monte Carlo procedure is employed to decide whether to stay on the same surface or hop to a different surface at each step in every trajectory.

If the steps are short, a good two-state approximation for  $B_{jk}^{(m)}$ , which takes into account that  $\boldsymbol{\eta}_{ij}$  can be quite large in the avoided crossing region, is  $B_{jj}^{(m)} = \exp(iS_j/\hbar) \cos(\Delta\theta_\tau)$  and  $B_{jk}^{(m)} = \exp(iS_{jk}/\hbar) \sin(\Delta\theta_\tau)$ , where  $\Delta\theta_\tau = \int d\mathbf{r} \cdot \boldsymbol{\tau}_{jk}$  with the integration taken across the step.<sup>29</sup> This short step approximation for  $B_{jj}^{(m)}$  treats the phase  $S_j$  as the same for all trajectories for this step that start and end in state  $\varphi_j$  (i.e., that have 0, 2, 4, ... hops), and it sums the corresponding terms in surface hopping wave function expansion within this approximation. Likewise, the short step approximation for  $B_{jk}^{(m)}$ , with  $k \neq j$ , sums all terms with an odd number of hops during the step within the approximation that the action  $S_{jk}$  is the same for all terms. The action  $S_j$  is evaluated for the trajectory segment with no hop during the step, and  $S_{jk}$  is evaluated for the trajectory segment with a hop in the middle of the step. In the calculations presented below, a higher order approximation<sup>34–36</sup> for  $B_{jj}^{(m)}$  and  $B_{jk}^{(m)}$  is used. This higher order approximation accounts for the dependence of the phase on the position of the hop or hops during the step. The use of the higher order step amplitudes allows for longer step lengths, which reduces the statistical error in the Monte Carlo calculation for a certain size sample.<sup>34–36</sup>

The surface hopping propagator can be expressed in the initial value representation<sup>41,42</sup> as

$$K_{ij}(\mathbf{x}_i, \mathbf{x}_f, t) = \int d\mathbf{p}_0 D K_{ij}(\mathbf{x}_0, \mathbf{x}_i, t) \delta(\mathbf{x}_t - \mathbf{x}_f) \quad (5)$$

where  $D = \|\partial \mathbf{x}_t / \partial \mathbf{p}_0\|$  and  $\mathbf{x}_t$  is the position at time  $t$  of the trajectory starting at  $\mathbf{x}_0$  and  $\mathbf{p}_0$ . The probability of a transition from state  $\varphi_i$  to state  $\varphi_f$  is given by

$$\begin{aligned} P_{ij}(t) &= \int d\mathbf{x}_f \int d\mathbf{x}_{0a} \int d\mathbf{x}_{0b} K_{ij}(\mathbf{x}_{0a}, \mathbf{x}_f, t) K_{ij}(\mathbf{x}_{0b}, \mathbf{x}_f, t)^* \\ &\quad \rho_0(\mathbf{x}_{0a}, \mathbf{x}_{0b}) \\ &= \int d\mathbf{p}_{0a} \int d\mathbf{p}_{0b} \int d\mathbf{x}_{0a} \int d\mathbf{x}_{0b} K_{ij}(\mathbf{x}_{0a}, \mathbf{x}_{ta}, t) \\ &\quad K_{ij}(\mathbf{x}_{0b}, \mathbf{x}_{tb}, t)^* \rho_0(\mathbf{x}_{0a}, \mathbf{x}_{0b}) D_a D_b \delta(\mathbf{x}_{ta} - \mathbf{x}_{tb}) \end{aligned} \quad (6)$$

where the  $\mathbf{x}_f$  integration has been performed giving the  $\delta(\mathbf{x}_{ta} - \mathbf{x}_{tb})$  factor from the  $\delta(\mathbf{x}_{ta} - \mathbf{x}_f)$  and  $\delta(\mathbf{x}_{tb} - \mathbf{x}_f)$  factors and  $\rho_0(\mathbf{x}_{0a}, \mathbf{x}_{0b})$  is the density of the initial system.

Calculations are presented in the next section for a one-dimensional curve crossing problem with  $\rho_0(x_a, x_b) = \psi_0(x_a)\psi_0(x_b)^*$  and  $\psi_0(x) = (2\gamma/\hbar\pi)^{1/4} \exp[-(\gamma/\hbar)(x - x_i)^2 + (i/\hbar)p_i(x - x_i)]$ . This is a scattering problem, and it is the long time limit of the transition probability that is evaluated. The time that it takes for a given trajectory to get from a point  $x_0$  in the incoming asymptotic region to the point  $x_f$  in the final asymptotic region depends on the sequence of hops. If more time during the trajectory is spent in the lower energy adiabatic state, then it takes less time to cross the interaction region and reach  $x_f$ . In the long time limit, a small change in the initial momentum makes a very large change in the final position. In

this case, the  $D_b \delta(x_{ta} - x_{tb})$  factor in eq 6 can be approximated as  $\delta(p_{0a} - p_{0b})$ , using  $\partial p_i / \partial x_0 = \partial^2 S / \partial x_i \partial x_t = -\partial p_0 / \partial x_t$ , giving

$$P_{ij}(t) = \int dp_{0a} \int dx_{0a} \int dx_{0b} K_{ij}(x_{0a}, x_{ta}, t) K_{ij}(x_{0b}, x_{tb}, t)^* D_a \rho_0(x_{a0}, x_{b0}) \quad (7)$$

where the  $p_{0b}$  integration is eliminated by the  $\delta(p_{0a} - p_{0b})$  factor.

The phase factor in this expression contains the  $p_i(x_{0a} - x_i)$  and  $p_i(x_{0b} - x_i)$  phases from  $\psi_0$  and  $\psi_0^*$  and  $S_a$  and  $S_b$  phases from the actions of the trajectories

$$\begin{aligned} \xi &= p_i(x_{a0} - x_i) - p_i(x_{b0} - x_i) + S_a - S_b \\ &= (p_i - p_{a0})(x_{a0} - x_i) - (p_i - p_{b0})(x_{b0} - x_i) \\ &\quad + p_{a0}(x_{a0} - x_i) - p_{b0}(x_{b0} - x_i) + S_a - S_b \end{aligned} \quad (8)$$

In the long time limit,  $|p_{a0} - p_{b0}| \sim 1/t$  and  $|E_a - E_b| \sim 1/t^2$ . Therefore,  $S_a - S_b = W_a - W_b$  in eq 8, where  $W = \int p \, dr = S + Et$ , and the integration is over the trajectory. Since  $\partial W_a / \partial x_{a0} = -p_{a0}$ ,  $\partial[W_a + p_{a0}(x_{a0} - x_i)] / \partial x_{a0} = 0$ , and similarly  $[W_b + p_{b0}(x_{b0} - x_i)] / \partial x_{b0} = 0$ . Thus, the  $a$  ( $b$ ) trajectory can be started at  $x_i$  rather than  $x_{a0}$  ( $x_{b0}$ ) without changing the last four terms in  $\xi$ . When  $W_a$  and  $W_b$  are calculated along these trajectories starting at  $x_i$ ,  $\xi$  is given by

$$\xi = (p_i - p_{a0})(x_{a0} - x_i) - (p_i - p_{b0})(x_{b0} - x_i) + W_a - W_b \quad (9)$$

$W_a$  and  $W_b$  have different values, since they are over trajectories with different sequences of hops and different positions of the hops. Since the two long time trajectories are very similar, except in the interaction region (which becomes a smaller and smaller fraction of the trajectories as  $t \rightarrow \infty$ ),  $A_a A_b^* D_a = (2\pi\hbar)^{-d} \|\partial p_0 / \partial x_t\|_a^{1/2} \|\partial p_0 / \partial x_t\|_b^{1/2} \|\partial x_t / \partial p_0\|_a \approx (2\pi\hbar)^d$  in the long time limit, where the  $A$ 's are the propagator prefactors and  $\partial^2 S / \partial x_0 \partial x_t = -\partial p_0 / \partial x_t$  has been used. Performing the  $x_{a0}$  integration in eq 7 gives  $\alpha_i(p_{a0}) = \int (2\gamma/\hbar\pi)^{1/4} \exp[-(\gamma/\hbar)(x_{a0} - x_i)^2 + (i/\hbar)(p_i - p_{a0})(x_{a0} - x_i)] dx_{a0} = (2\pi\hbar/\gamma)^{1/4} \exp[-(p_i - p_{a0})^2/4\gamma\hbar]$ , where the  $(p_i - p_{a0})(x_{a0} - x_i)$  phase factor comes from eq 9. The  $x_{b0}$  integration gives the complex conjugate of this result. Equation 7 can now be written in the form

$$P_{ij} = \int |a_i(p_0)|^2 |a_{ij}(p_0)|^2 dp_0 \quad (10)$$

where  $a_{ij}(p_0)$  is the amplitude (i.e., the wave function divided by its prefactor) for the semiclassical surface hopping wave function corresponding to an initial momentum  $p_0$  and the  $W$  phase function is evaluated starting at  $x_i$  in the incoming asymptotic region and ending at  $x_j$  in the outgoing asymptotic region. An alternate derivation, which is based on the time independent surface hopping wave function and shows that the cancelation that removed the prefactors is exact in this case, is given in the Appendix. The Monte Carlo procedure used to evaluate  $P_{ij}$  is described in detail in the next section.

### III. CALCULATIONS

**A. Method.** In this section, surface hopping calculations are presented for the one-dimensional, two-state problems defined by the diabatic states

$$V_{11}(x) = A_{11} \tanh[a_{11}(x - x_c)] \tanh[a_{11}(x + x_c)] \quad (11a)$$

$$V_{22}(x) = -V_{11}(x) \quad (11b)$$

$$V_{12}(x) = A_{12} \exp(-a_{12}x^2) \quad (11c)$$

where  $A_{11} = 1.0$ ,  $a_{11} = 1.0$ ,  $x_c = 2.0$ ,  $A_{12} = 0.1$ , and  $a_{12} = 0.05$ . The particle mass is taken to be 1836.0, and  $\hbar = 1$ . The diabatic surfaces are shown in Figure 1. The symmetric matrix formed

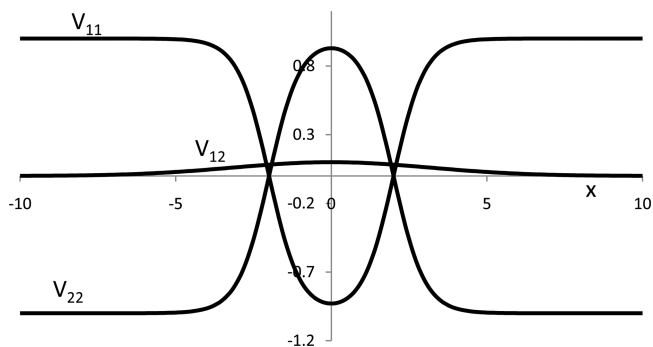


**Figure 1.** The diabatic surface used in the calculations,  $V_{11}(x)$ ,  $V_{22}(x)$ , and  $V_{12}(x)$ .

from the  $V_{ij}$  is diagonalized to give the adiabatic states energies,  $U_1$  and  $U_2$ , and the corresponding adiabatic states can be expressed as

$$\varphi_1(x) = \cos(\theta)\varphi_1^{(d)} + \sin(\theta)\varphi_2^{(d)} \quad (12a)$$

$$\varphi_2(x) = -\sin(\theta)\varphi_1^{(d)} + \cos(\theta)\varphi_2^{(d)} \quad (12b)$$

where the  $\varphi_j^{(d)}$  are the diabatic states and  $\theta = 1/2 \tan^{-1}[2V_{12}/(V_{11} - V_{22})]$ . The nonadiabatic coupling is given by  $\eta_{12} = \langle \varphi_2 | d\varphi_1/dx \rangle = d\theta/dx$ , where  $\langle \dots \rangle$  denotes integration over the electronic coordinates. The diabatic surfaces cross at  $x_c$  and  $-x_c$ , similar to Tully's test problem II.<sup>14</sup> The initial density is given by  $\rho_0(x_a, x_b) = \psi_0(x_a)\psi_0(x_b)^*$ , where the initial wave function is  $\psi_0(x) = (2\gamma/\pi\hbar)^{1/4} \exp[-(\gamma/\hbar)(x - x_i)^2 + (i/\hbar)p_i(x - x_i)]$ .

The  $a_{ij}(p_0)$  amplitudes are calculated using eq 9 for the phase by taking finite size steps in  $x$  from  $x_i$  in the incoming asymptotic region to a point in the outgoing asymptotic region,  $x_f$ . The wave function amplitudes for either staying on the same adiabatic surface or for hopping to the other adiabatic surface are calculated for each of the hopping steps. These hopping steps are typically much longer than the step size used for the integration of the trajectories and the integrals needed in the calculations. In this work, the higher order amplitudes presented previously are employed for each hopping step. These amplitudes for a step starting at  $x_s$  and ending at  $x_e$  have the form<sup>34</sup>

$$B_{11} = \exp\left[\frac{i}{\hbar}(W_{11} + \chi_a)\right] \cos(\gamma) \quad (13)$$

$$B_{12} = \exp\left[\frac{i}{\hbar}W_{12}\right] \sin(\gamma) \quad (14)$$

$$B_{21} = -\exp\left[\frac{i}{\hbar}W_{21}\right] \sin(\gamma) \quad (15)$$

$$B_{22} = \exp\left[\frac{i}{\hbar}(W_{22} - \chi_a)\right] \cos(\gamma) \quad (16)$$

where

$$\gamma = \int_{x_s}^{x_e} dx_1 \tau_{12}(x_1) \cos\left(\frac{1}{\hbar} \int_{x_s}^{x_1} [p_2(x) - p_1(x)] dx\right) \quad (17)$$

$$\chi_a = -\frac{i}{\hbar} \int_{x_s}^{x_e} dx_1 \tau_{12}(x_1) \int_{x_1}^{x_e} dx_2 \tau_{12}(x_2) \int_{x_1}^{x_2} dx (p_2 - p_1) \quad (18)$$

$$W_{ij} = \int_{x_s}^{x_a} p_i dx + \int_{x_a}^{x_e} p_j dx \quad (19)$$

and  $x_a$  is determined by the condition

$$\int_{x_s}^{x_e} dx_1 \tau_{12}(x_1) \int_{x_a}^{x_1} (p_2 - p_1) dx = 0 \quad (20)$$

The total amplitude for the  $i \rightarrow f$  transition,  $a_{if}(p_0)$ , can be expressed as the summation over all possible sequences of hops and nonhops for all the steps from  $x_0$  to  $x_f$  and the contribution from each of these sequences is just the product of the appropriate  $B_{ij}$  step amplitudes

$$a_{if}(p_0) = \sum_a \prod_m B_{j_{am}k_{am}}^{(m)} \quad (21)$$

where  $m$  labels the steps, the subscript  $j$  specifies the adiabatic state at the beginning of the step, and  $k$  specifies the adiabatic state at the end of the step as determined by the Monte Carlo hopping procedure. The summation is over all possible sequences of hopping and nonhopping in the different hopping steps between  $x_i$  and  $x_f$ . A Monte Carlo sampling of sequences of hops and nonhops for eq 21 must be used in many dimensional problems, and it is used in this work. At each step, the Monte Carlo probability of hopping from the current state,  $\varphi_i$ , to the other state,  $\varphi_j$ , is taken to be  $p_{jk} = |B_{jk}|/(|B_{jk}| + |B_{ji}|)$ , and the probability for not hopping is taken to be  $p_{jj} = |B_{ji}|/(|B_{jk}| + |B_{ji}|)$ . Given these probabilities,  $B_{jk} = \text{sgn}(B_{jk})B_{jk}$  and  $B_{ji} = \text{sgn}(B_{ji})B_{ji}$ , where  $B = |B_{jk}| + |B_{ji}|$ . Since  $p_{jk}$  and  $p_{jj}$  are the probabilities used in the hop/nonhop decision, this Monte Carlo procedure averages the products of the quantities  $g_{jk} = \text{sgn}(B_{jk})B$  and  $g_{ji} = \text{sgn}(B_{ji})B$  from each step in both trajectories to get the transition probabilities

$$P_{if} = \frac{1}{N_s} \sum_{a=1}^{N_f} \prod_m g_{j_{1am}k_{1am}}^{(m)} g_{j_{2am}k_{2am}}^{(m)*} \quad (22)$$

with the subscripts 1 and 2 indicating the two trajectories. The sum in eq 22 is over all samplings in which both trajectories are in state  $\varphi_i$  at  $t = 0$  and in state  $\varphi_f$  at the final time,  $N_s$  is the number of Monte Carlo samplings, and  $N_f$  is the number of samplings ending in state  $\varphi_f$ .

The Monte Carlo calculations for the transition probabilities are carried out as follows. For each trajectory pair in the Monte Carlo calculation, a value of  $p_0$  is sampled from the  $\rho_p(p_0) = |\alpha_i(p_0)|^2$  factor in eq 10. Two methods for sampling  $p_0$  are compared. The first method directly samples  $p_0$  using random numbers between 0 and 1. The second method selects the values of  $p_0$  using a Sobol sequence<sup>37–40</sup> of numbers between 0 and 1. Once the Sobol number is obtained, the value of  $p_0$  is evaluated using a numerical approximation<sup>43</sup> to the inverse of the cumulative probability distribution. Once  $p_0$  has been selected, the two hopping trajectories, which start at  $x_i$  with the same energy, are evaluated. Hops are not attempted in regions where the nonadiabatic coupling is small. In the calculations performed here, the angle  $\Delta\theta(x) = \int_{x_0}^x \eta_{ij} dx$  is evaluated along the trajectories. Hops are attempted only in regions where  $\varepsilon <$

$|\Delta\theta| < \pi/2 - \varepsilon$ , where  $\varepsilon$  is a small number. The fact that hops are not attempted in regions where the coupling is small saves the computational time required for averaging over different trajectory segments in these small coupling regions. For the system considered here, there is a region,  $x_{L-} < x < x_{U-}$ , where hopping is attempted for  $x < 0$  and an equivalent region,  $x_{L+} < x < x_{U+}$ , for  $x > 0$ . These hopping regions are divided into a number of hopping steps, and the  $B_{ij}$  hopping amplitudes are evaluated in each of these hopping steps.

At each hopping step along each trajectory, a uniformly distributed random number,  $0 < \zeta < 1$ , is generated. If  $p_{ab} \geq \zeta$ , then a hop is made to the other adiabatic surface during the step, and if  $p_{ab} < \zeta$ , the trajectory stays on the same adiabatic surface. The corresponding amplitude  $g_{j_{m}k_{m}}^{(m)}$  is evaluated for that step.

In order to improve the numerical efficiency of the Monte Carlo calculation, local averaging is performed across each of the interaction regions,  $x_{L-} < x < x_{U-}$  and  $x_{L+} < x < x_{U+}$ . When a trajectory reaches the lower boundary of an interaction region,  $n$  versions of it are continued through the interaction region, each with a different randomly chosen set of hops and nonhops. The amplitude for the segment is just the product of the  $g_{j_{m}k_{m}}^{(m)}$  amplitudes for each step within the segment. The average of the segment amplitudes over the  $n$  trajectory segments provides the amplitude for the interaction region

$$h_{j,K}^{(M,q)} = \frac{1}{n} \sum_{b=1}^{n_c} \prod_m g_{j_{bm}k_{bm}}^{(m)} \quad (23)$$

where  $J$  ( $K$ ) is the state of the system at the beginning (end) of the interaction region,  $M$  indicates whether this is the first or second interaction region,  $q$  indicates whether this is trajectory 1 or 2 in the trajectory pair, and the product is taken over the hopping steps within the interaction region. The summation includes only the trajectory segments that are in state  $\varphi_K$  at the end of the interaction region.

After the first interaction region has been crossed, trajectories are continued on both surfaces, and the contributions to the  $W_j = \int p_j dx$  phase functions are evaluated. When the second interaction region is reached,  $n$  trajectory segments are started on each of the two surfaces at the beginning of the interaction region and continued with a hop or no hop during each hopping step until the end of the interaction region is reached. The amplitudes obtained for each trajectory segment are used to evaluate the averaged  $h_{j,K}^{(M,q)}$  factors for the second hopping region. There are two contributions to the wave function amplitude corresponding to starting in state  $\varphi_1$  at  $x_i$  and being in state  $\varphi_K$  at the end of the second interaction region, and these are summed. If state  $K$  is  $\varphi_2$ , then the two contributions change state in one interaction region but not in the other, and they differ in which interaction region the state change occurs. On the other hand, if state  $K$  is  $\varphi_1$ , then one of the contributions changes state in neither interaction region and the other changes state in both interaction regions. Trajectories are continued on both surfaces from the end of the second interaction regions to the final point  $x_f$  in the outgoing asymptotic region. Using these average contributions to the wave function, the transition probability,  $P_{ij} = \int \rho(p_0) |\psi_{ij}(x_f, p_0)|^2 dp_0$ , can be expressed as



$$P_{if} = \frac{1}{N_s} \sum_{a=1}^{N_s} \left[ \sum_{K_1=1}^2 \sum_{K_2=1}^2 h_{i,K_1}^{(1,1)} h_{K_1,f}^{(2,1)} h_{i,K_2}^{(1,2)} h_{K_2,f}^{(2,2)} e^{i(w_{(1,K_1)} - w_{(2,K_2)})/\hbar} \right]_a \quad (24)$$

where  $N_s$  is the number of  $p_0$  values sampled,  $w_{j,K}$  is the contribution to the phase function  $W$  from the portions of trajectory  $j$  ( $j = 1, 2$ ) outside the interaction regions, and  $K_i$  is the state for the system at the end of the first interaction region for the  $i$ th trajectory of the trajectory pair ( $i = 1, 2$ ).

The results from calculations are shown in Table 1. These calculations differ in the numbers of trajectory pairs,  $N$ , and in

**Table 1. RMS Errors in Monte Carlo Surface Hopping Transition Probabilities<sup>a</sup>**

$N$	$n$	$\Delta X$	$\varepsilon$	$\Delta\Theta$	$\sigma(S)$	$\sigma(R)$	effort
50	10	0.5	$0.03\pi$	0.9	0.0546	0.0553	102
50	20	0.25	$0.03\pi$	0.9	0.0435	0.0529	160
50	30	0.25	$0.03\pi$	0.9	0.0377	0.0474	218
50	40	0.25	$0.025\pi$	0.7	0.0354	0.0444	276
50	50	0.25	$0.025\pi$	0.7	0.0343	0.0378	334
50	60	0.25	$0.025\pi$	0.7	0.0244	0.0464	392
100	10	0.5	$0.03\pi$	0.9	0.0498	0.0511	204
100	20	0.25	$0.03\pi$	0.9	0.0406	0.0384	320
100	30	0.25	$0.025\pi$	0.7	0.0219	0.0336	436
100	40	0.25	$0.025\pi$	0.7	0.0229	0.0298	552
100	50	0.25	$0.025\pi$	0.7	0.0230	0.0244	668
100	60	0.25	$0.025\pi$	0.7	0.0157	0.0271	784
200	10	0.25	$0.025\pi$	0.7	0.0412	0.0434	409
200	20	0.25	$0.025\pi$	0.7	0.0279	0.0244	641
200	30	0.25	$0.025\pi$	0.7	0.0194	0.0243	873
200	40	0.25	$0.025\pi$	0.7	0.0168	0.0226	1105
200	50	0.25	$0.025\pi$	0.7	0.0147	0.0194	1337
200	60	0.25	$0.025\pi$	0.7	0.0136	0.0171	1569
400	20	0.25	$0.025\pi$	0.7	0.0217	0.0237	1282
400	30	0.25	$0.025\pi$	0.7	0.0153	0.0156	1746
400	40	0.25	$0.025\pi$	0.7	0.0123	0.0151	2210
400	50	0.25	$0.025\pi$	0.7	0.0111	0.0160	2673
400	60	0.25	$0.025\pi$	0.7	0.0098	0.0137	3738

<sup>a</sup> $\sigma(S)$  is the RMS error when a Sobol sequence is used for the momentum sampling, and  $\sigma(R)$  is the corresponding quantity when a random number generator is employed.  $N$  is the number of trajectories run in a given calculation, and  $n$  is the number of copies of that trajectory averaged across each hopping region. The effort is the number of trajectories with  $n = 1$  that have a roughly equivalent computational effort to the  $N$  trajectory calculation with the given value of  $n$ .  $\Delta X$ ,  $\varepsilon$ , and  $\Delta\Theta$  determine the width of the interaction region and hopping steps (see text for details).

$n$ , the number of copies of a given trajectory used for averaging the wave function amplitude for an interaction region. The results of these calculations also depend on the choice of  $\varepsilon$ , which defines the strong interaction region, as described in section III.A. The higher order amplitudes, eqs 13–16, are derived by approximating the contributions from the full surface hopping wave function expansion.<sup>34</sup> These approximations introduce an error of order  $(\Delta x)^4$ , where  $\Delta x$  is the width of the hopping step. This width for each hopping step is chosen such that  $\Delta x$  is no larger than a set maximum,  $\Delta X$ , and that the value of  $\Delta\Theta$  is no larger than a set maximum,  $\Delta\Theta$ , where  $\Delta\Theta$  is the integral of  $|\eta_{ij}|$  across the step. All trajectories

are run between  $x_0 = -10$  and  $x_f = 10$ . The effort per trajectory pair is greater than it would be for a simple trajectory pair due to the averaging over trajectory segments within the integration regions. While the width of the interaction regions varies a little depending on the value of  $\varepsilon$ , the sum of widths of the two interaction regions is always around 11.6% of the total length of the trajectories. Thus, the effort to integrate a trajectory can be approximated as  $0.884 + 0.116n$ , so that an  $N$  trajectory pair calculation is roughly equivalent to  $(0.884 + 0.116n)N$  trajectory pairs.

Calculations are performed for 91 values of the average momentum for  $\psi_0(x)$ . These values of  $p_0$  correspond to evenly spaced values of the energy between 1.5 and 6.0. Exact quantum calculations are also performed for these initial wave functions using the fast Fourier transform split operator approach.<sup>44</sup> After each surface hopping calculation with a given  $\psi_0$ , the probabilities for ending in adiabatic state  $\varphi_1$ ,  $P_{11}$ , and for ending in state  $\varphi_2$ ,  $P_{12}$ , are multiplied by a constant so that  $P_{11} + P_{12} = 1$ . This reduces the random error in the calculations somewhat. The  $\sigma$  values reported in the table are the root mean squared (RMS) error of the  $P_{11}$  and  $P_{12}$  values compared with the quantum results,  $P_{11}^Q$  and  $P_{12}^Q$ , for the  $N_c = 91$  energies.

$$\sigma^2 = \frac{1}{2N_c} \sum_{i=1}^{N_c} [(P_{11} - P_{11}^Q)^2 + (P_{12} - P_{12}^Q)^2] \quad (25)$$

The results presented in the table show that good accuracy results can be obtained using the surface hopping expansion with a modest number of trajectories. For each set of calculations, values are given for  $\varepsilon$ , which determines how wide the interaction regions are, and for  $\Delta X$  and  $\Delta\Theta$ , which determine the width of the hopping steps. The values of these parameters are the same for most calculations, although they are adjusted to make the interaction region a little smaller and the hopping steps a little larger in calculations with the smaller values of  $N$  and  $n$ , since this improves the accuracy of calculations with small sample sizes.

When a Sobol sequence is used for the sampling of the momentum, the RMS error in the probabilities for hopping and not hopping can be reduced to under 0.05 using 50 trajectories, if the wave function is averaged over 20 different hopping histories in each interaction region. When the additional effort for running these histories is accounted for, the effort for this simulation is roughly equivalent to running about 160 trajectory pairs. The error is reduced to less than 0.04 if the number of different hopping histories averaged over when crossing each interaction region is increased to 30, in which case the overall effort is equivalent to running a bit under 280 trajectory pairs. It can be brought to under 0.03 with an effort equivalent to a little less than 400 trajectory pairs and to under 0.02 with an effort similar to a simulation with about 875 trajectory pairs. If a random number generator is used to sample the initial momentum, the corresponding numbers of equivalent trajectory pairs are as follows: a little over 200 for an error under 0.05, under 350 for an error below 0.04, around 550 for an error of 0.03, and less than 1350 for an error that is less than 0.02.

## IV. DISCUSSION

The results presented show significant improvement in efficiency over those obtained in earlier work,<sup>35,36</sup> which did not include the averaging in the interaction regions. In the

previous work, an error of about 0.02 was obtained in calculations with 10 000 trajectories. Figure 2 shows the

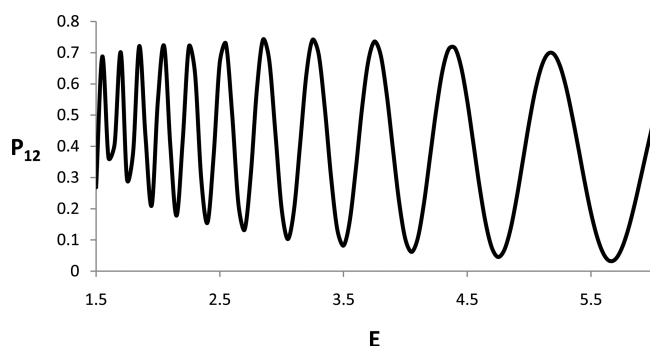


**Figure 2.** The long time quantum transition probability  $P_{12}$  as a function of  $E = p_i^2/2m + U_i(x_i)$  corresponding to the initial wave function  $\psi_0(x) = (2\gamma/\pi\hbar)^{1/4} \exp[-(\gamma/\hbar)(x - x_i)^2 + (i/\hbar)p_i(x - x_i)]$ .

quantum transition probability  $P_{12}^Q(E)$ . There is significant quantum interference resulting in the oscillations in the transition probability. The surface hopping method is clearly capable of reproducing this quantum interference given the high level of accuracy achieved.

There are two types of errors in these calculations, sampling error and error due to numerical approximations. The error due to numerical approximations in the higher order step amplitudes can be reduced by choosing a shorter length for each hopping step. However, this increases the number of steps needed to cross each interaction region. This results in greater cancelation between different hopping histories across an interaction region, producing a higher statistical error for fixed values of  $N$  and  $n$ . This increased statistical error can be offset by increasing  $N$  and  $n$ .

In this work, the distribution for the initial momentum is sampled directly. This provides a better comparison with earlier work, which did not include the averaging of hopping histories across the interaction regions. Multidimensional problems would, in all likelihood, require the use of a Metropolis Monte Carlo procedure for selecting the trajectory pairs. Changing variables in eq 6 from  $\mathbf{p}_{0b}$  to  $\mathbf{x}_{tb}$  and from  $\mathbf{x}_{b0}$  to  $\mathbf{p}_{tb}$ , the following expression is obtained after the integration over  $\mathbf{x}_{tb}$

$$P_{ij}(t) = \int d\mathbf{p}_{tb} \int d\mathbf{x}_{0a} \int d\mathbf{p}_{0a} K_{ij}(\mathbf{x}_{0a}, \mathbf{x}_t, t) K_{ij}(\mathbf{x}_{0b}, \mathbf{x}_t, t)^* D_a D_b \rho_0(\mathbf{x}_{a0}, \mathbf{x}_{b0}) \quad (26)$$

Equation 26 can be used in a forward–backward calculation.<sup>45–60</sup> A Monte Carlo procedure is employed to choose the  $\mathbf{x}_{0a}$  and  $\mathbf{p}_{0a}$  for the forward trajectory. This forward trajectory is integrated, and a Monte Carlo decision to stay on the same surface or to hop to a different surface is made for each step along the trajectory. After the forward trajectory has been integrated to time  $t$  in this manner, the final momentum for the backward trajectory,  $\mathbf{p}_{tb}$ , is selected by a Metropolis Monte Carlo procedure, and this trajectory is run backward in time to time zero. The Metropolis accept/reject decision would be weighted by the initial density  $\rho_0(\mathbf{x}_{a0}, \mathbf{x}_{b0})$ .

In the forward–backward expression for the multidimensional transition probability, eq 26, the prefactor for the propagator,  $K_\gamma$ , is proportional to  $D_\gamma^{-1/2}$ , where  $\gamma = a, b$ . The calculation of these factors is problematic in high dimensional

problems. The prefactors and  $D$  factors can be eliminated using Miller's linearized semiclassical initial value representation (LSC-IVR).<sup>60</sup> The LSC-IVR method would not accurately account for quantum interference between trajectories hopping during different crossings of strong interaction regions. This type of interference produces the oscillations in Figure 2 in this work. In high dimensional problems, this type of interference becomes much less important because of the decoherence resulting from phase interference between the contributions from the various possible paths between the different crossings of strong interaction regions. On the other hand, the *local* interference between paths with different hopping histories during a *single* crossing of a strong coupling region is still important and can be accounted for by averaging trajectories with different histories in this region, as is done in this work. This should result in an accurate and efficient method for high dimensional problems. In lower dimensional problems in which quantum interference is important, it will be necessary to use eq 26 and calculate the prefactors.

It is quite common in multidimensional problems that the interstate coupling is localized near an avoided crossing seam or a conical intersection. In such problems, it should be possible to average over multiple copies of the portion of the trajectory corresponding to crossing these strong coupling regions. In the current work, the strong coupling region was defined in terms of  $\theta = \int \eta dx$  where the integral is taken along the trajectory. This can be easily generalized for multidimensional problems, although care must be taken near conical intersections. Alternatively, the strong coupling region can be defined in terms of  $|\eta|$ . The implementation for multidimensional problems is complicated by the fact that trajectories hopping at different points within the strong coupling region will have different positions and momenta at the end of the strong coupling region. However, it should still be possible to average over these trajectories, as is done in the one-dimensional case considered here, as long as the strong coupling region is not too wide. A single trajectory can then be continued from the end of the average trajectory. In the case of a wide region, it may be better to divide this region into two or more subregions, and average within each of these. Furthermore, hopping and nonhopping trajectories will continue in different directions after the end of a strong coupling region in multidimensional calculations. The Monte Carlo procedure would have to decide which branch or branches of the trajectory would be continued after a strong couple region is crossed. The extension of the averaging technique and the higher order amplitudes used in this work to multidimensional problems is the topic of current research.

The calculation of the higher order amplitudes in one dimension only requires the calculation of a few extra integrals across the hopping step length. In many dimensions, trajectories hopping at different points in the hopping step have different end points. The calculation of higher order amplitudes in this case will certainly require the integration of a number of hopping trajectories within each hopping step. In addition, a Metropolis sampling procedure will be needed for the forward–backward trajectory pairs, and this will be less efficient than the sampling used in this work. Even if the increase in effort due to these considerations is about an order of magnitude or a little more, this would still result in being able to obtain  $P_{ij}(t)$  with errors on the order of 0.05 with an effort equivalent to a few thousand trajectory pairs. If a higher

accuracy than 0.05 is needed, this can, of course, be obtained at the expense of running more trajectory pairs.

## APPENDIX

### The Derivation of eq 10 Using Time Independent Surface Hopping Wave Functions

In this appendix, an alternate derivation of eq 10 for the one-dimensional transition probability is given. The propagator can be expressed as the integral over time independent states

$$\mathbf{K}(x_0, x, t) = \frac{1}{2\pi\hbar} \int dp_0 \psi(x, p_0) \psi(x_0, p_0)^\dagger e^{-iEt/\hbar} \quad (\text{A1})$$

where  $E = p_0^2/2m + U_i$ . In eq A1,  $\psi(x, p_0)$  is a column in which the  $j$ th element is the state  $\varphi_j$  component of the time independent surface hopping wave function<sup>29</sup> that started in state  $\varphi_i$  as a plane wave in the incoming asymptotic region. The  $\varphi_i$  to  $\varphi_f$  component of the time dependent wave function is given by  $\psi_{if}(x, t) = \int \langle \varphi_f | \mathbf{K}(x_0, x, t) | \varphi_i \rangle \psi_0(x_0) dx_0 = (2\pi\hbar)^{-1/2} \int dp_0 \psi_{if}(x, p_0) \alpha(p_0) e^{-iEt/\hbar}$ , where  $\alpha(p_0) = (2\pi\hbar)^{-1/2} \int \psi_0(x_0) \exp(-ip_0 x_0/\hbar) dx_0$  and the fact that  $\psi_0(x_0) = \exp(-ip_0 x_0/\hbar)$  has been used. The transition probability,  $P_{if}(t) = \int \psi_{if}(x, t) \psi_{if}(x, t)^* dx$ , can be expressed as

$$P_{if}(t) = (2\pi\hbar)^{-1} \int dx \int dp_{a0} \int dp_{b0} \psi_{if}(x_f, p_{a0}) \psi_{if}(x_f, p_{b0})^* \alpha_{if}(p_{a0}) \alpha_{if}(p_{b0})^* \exp\{i[(p_{fa} - p_{fb}) \cdot (x - x_f) - i(E_a - E_b)t]/\hbar\} \quad (\text{A2})$$

where the fact that  $\psi_{if}(x, t) = \psi_{if}(x_f, t) \exp[ip_f(x - x_f)]$  in the final asymptotic region has been employed. Performing the  $x$  integration, and then making the substitution  $\delta(p_{fa} - p_{fb}) = (p_{fa}/p_{a0})\delta(p_{a0} - p_{0b})$  and performing the  $p_{a0}$  integration, the final result is obtained

$$P_{if}(t) = \int dp_{a0} \int dp_{b0} \psi_{if}(x_f, p_{a0}) \psi_{if}(x_f, p_{b0})^* a_{if}(p_{a0}) a_{ij}(p_{b0})^* \delta(p_{fa} - p_{fb}) = \int dp_0 |a_{if}(x_f, p_0)|^2 |\alpha(p_0)|^2 \quad (\text{A3})$$

where  $a_{if}(x_f, p_0) = (p_f/p_0)^{1/2} \psi_{if}(x_f, p_0)$ . Note that  $P_{if}(p_0)$ , the probability of the system being in a specific final state for a time independent system at energy  $E(p_0)$ , is given by the ratio of the final flux over the initial flux, so that  $|a_{if}(x_f, p_0)|^2 = (p_f/p_0) |\psi_{if}(x_f, p_0)|^2 = P_{if}(p_0)$ . The flux ratio,  $p_f/p_0$ , cancels the prefactors in  $|\psi_{if}(x_f, p_0)|^2$ , which shows that the cancelation of the prefactors is exact in the one-dimensional case.

## AUTHOR INFORMATION

### Notes

The authors declare no competing financial interest.

## REFERENCES

- (1) Nikitin, E. E. *Theory of Elementary Atomic and Molecular Processes in Gases*; Oxford University: London, 1974.
- (2) Nakamura, H. *Nonadiabatic Transitions: Concepts, Basic Theories, and Applications*; World Scientific: Singapore, 2002.
- (3) Delos, J. B.; Thorson, W. R. Studies of the Potential-Curve-Crossing Problems II. General Theory and a Model for Close Crossing. *Phys. Rev. A* **1972**, *6*, 728–745.
- (4) Jasper, A. W.; Zhu, C.; Nangia, S.; Truhlar, D. G. Introductory Lecture: Nonadiabatic Effects in Chemical Dynamics. *Faraday Discuss.* **2004**, *127*, 1.
- (5) Zhu, C.; Jasper, A. W.; Truhlar, D. G. Non-Born-Oppenheimer Louville-von Neumann Dynamics. Evolution of a Subsystem Controlled by Linear and Population-Driven Decay of Mixing with Decoherent and Coherent Switching. *J. Chem. Theory Comput.* **2005**, *1*, 527–540.
- (6) Jasper, A. W.; Nangia, S.; Zhu, C.; Truhlar, D. G. Non-Born-Oppenheimer Molecular Dynamics. *Acc. Chem. Res.* **2006**, *39*, 101–108.
- (7) Li, B.; Chu, T.-S.; Han, K.-L. Non-Born-Oppenheimer Dynamics Calculations using Coherent Switching with Decay of Mixing Methods. *J. Comput. Chem.* **2010**, *31*, 362–370.
- (8) Meyer, H. D.; Miller, W. H. Analysis and Extension of Some Recently Proposed Classical Models for Electronic Degrees of Freedom. *J. Chem. Phys.* **1980**, *72*, 2272–2281.
- (9) Stock, G.; Thoss, M. Semiclassical Description of Nonadiabatic Quantum Dynamics. *Phys. Rev. Lett.* **1997**, *78*, 578–581.
- (10) Stock, G.; Thoss, M. Mapping Approach to the Semiclassical Description of Nonadiabatic Quantum Dynamics. *Phys. Rev. A* **1999**, *59*, 64–79.
- (11) Bonella, S.; Coker, D. F. Semiclassical Implementation of the Mapping Hamiltonian Approach for Nonadiabatic Dynamics Using Focused Initial Distribution Sampling. *J. Chem. Phys.* **2003**, *118*, 4370–4385.
- (12) Preston, R. K.; Tully, J. C. Effects of Curve Crossing in Chemical Reactions: The  $\text{H}_3^+$  System. *J. Chem. Phys.* **1971**, *54*, 4297–4304.
- (13) Tully, J. C.; Preston, R. K. Trajectory Surface Hopping Approach to Nonadiabatic Molecular Collisions: The Reaction of  $\text{H}^+$  with  $\text{D}_2$ . *J. Chem. Phys.* **1971**, *55*, 562–572.
- (14) Tully, J. C. Molecular Dynamics with Electronic Transitions. *J. Chem. Phys.* **1990**, *93*, 1061–1071.
- (15) Hammes-Shiffer, S.; Tully, J. C. Proton Transfer in Solution: Molecular Dynamics with Quantum Transition. *J. Chem. Phys.* **1994**, *101*, 4657–4667.
- (16) Burant, J. C.; Tully, J. C. Nonadiabatic Dynamics Via the Classical Limit Schrodinger Equation. *J. Chem. Phys.* **2000**, *112*, 6097–6103.
- (17) Fang, F.-Y.; Hammes-Shiffer, S. Comparison of Surface Hopping and Mean Field Approaches for Model Proton Transfer Reactions. *J. Chem. Phys.* **1999**, *110*, 11166–11175.
- (18) Webster, F.; Wang, E. T.; Rossky, P. J.; Friesner, R. A. Stationary Phase Surface Hopping of Nonadiabatic Dynamics. *J. Chem. Phys.* **1994**, *100*, 4835–4847.
- (19) Bittner, E. R.; Rossky, P. J. Decoherent Histories and Nonadiabatic Quantum Molecular Dynamics Simulations. *J. Chem. Phys.* **1997**, *107*, 8611–8618.
- (20) Ben-Nun, M.; Martinez, T. J. Nonadiabatic Molecular Dynamics: Validation of the Multiple Spawning Method for a Multidimensional Problems. *J. Chem. Phys.* **1998**, *108*, 7244–7257.
- (21) Yang, S.; Coe, J. D.; Kaduk, B.; Martinez, T. J. An “Optimal” Spawning Algorithm for Adaptive Basis Set Expansion in Nonadiabatic Dynamics. *J. Chem. Phys.* **2009**, *130*, No. 134113.
- (22) Hack, M. D.; Wensmann, A. M.; Truhlar, D. G.; Ben-Nun, M.; Martinez, T. J. Comparison of Full Multiple Spawning, Trajectory Surface Hopping, and Converged Quantum Mechanics for Electronically Nonadiabatic Dynamics. *J. Chem. Phys.* **2001**, *115*, 1172–1186.
- (23) Jasper, A. W.; Hack, M. D.; Truhlar, D. G. The Treatment of Classically Forbidden Electronic Transitions in Semiclassical Surface Hopping Calculations. *J. Chem. Phys.* **2001**, *115*, 1804–1816.
- (24) Jasper, A. W.; Stechmann, S. N.; Truhlar, D. G. Fewest Switches with Time Uncertainty: a Modified Trajectory Surface Hopping Algorithm with Better Accuracy for Classically Forbidden Electronic Transitions. *J. Chem. Phys.* **2002**, *116*, 5424–5431.
- (25) Jasper, A. W.; Truhlar, D. G. Improved Treatment of Momentum at Classically Forbidden Electronic Transitions in



Trajectory Surface Hopping Calculations. *Chem. Phys. Lett.* **2003**, 369, 60–67.

(26) Jasper, A. W.; Truhlar, D. G. Non-Born-Oppenheimer Dynamics of Na — FH Photodissociation. *J. Chem. Phys.* **2007**, 127, No. 194306.

(27) Nakamura, H. Nonadiabatic Chemical Dynamics: Comprehension and Control of Dynamics, and Manifestation of Molecular Functions. *Adv. Chem. Phys.* **2008**, 138, 95–212.

(28) Kondorshiy, A.; Nakamura, H. Semiclassical Theory of Electronically Nonadiabatic Chemical Dynamics: Incorporation of Zhu-Nakamura Theory into the Frozen Gaussian Propagation Method. *J. Chem. Phys.* **2004**, 120, 8937–8954.

(29) Herman, M. F. Generalization of the Geometric Optical Series Approach for Non-Adiabatic Scattering Problems. *J. Chem. Phys.* **1982**, 76, 2949–2958.

(30) Wu, W.; Herman, M. F. A Justification for a Nonadiabatic Surface Hopping Herman-Kluk Semiclassical Initial Value Representation of the time Evolution Operator. *J. Chem. Phys.* **2006**, 125, No. 154116.

(31) Wu, Y.; Herman, M. F. On the Properties of a Primitive Semiclassical Surface Hopping Propagator for Nonadiabatic Quantum Dynamics. *J. Chem. Phys.* **2007**, 127, No. 044109.

(32) Herman, M. F.; Wu, Y. An Analysis Through Order  $\hbar^2$  of a Surface Hopping Expansion for the Nonadiabatic Wave Function. *J. Chem. Phys.* **2008**, 128, No. 114105.

(33) M. F. Herman, M. F. Analysis of a Surface Hopping Expansion that Includes Hops in the Classically Forbidden Regions. *Chem. Phys.* **2014**, 433, 12–21.

(34) Moody, M. P.; Ding, F.; Herman, M. F. Phase Corrected Higher-Order Expressions for Surface Hopping Transition Amplitudes in Nonadiabatic Scattering Problems. *J. Chem. Phys.* **2003**, 119, 11048–11057.

(35) Herman, M. F.; Moody, M. P. Numerical Study of the Accuracy and Efficiency of Various Approaches for Monte Carlo Surface Hopping Calculations. *J. Chem. Phys.* **2005**, 122, No. 094104.

(36) Herman, M. F. Higher Order Phase Corrected Transition Amplitudes for Time Dependent Semiclassical Surface Hopping Calculations. *Chem. Phys.* **2008**, 351, 51–56.

(37) Brown, S. E.; Georgescu, I.; Mandelshtam, V. A. Self-Consistent Phonons Revisited. II. A General and Efficient Method for Computing Free Energies and Vibrational Spectra of Molecules and Clusters. *J. Chem. Phys.* **2013**, 138, No. 044317.

(38) Sobol, I. M. On the Distribution of Points in a Cube and The Approximate Evaluation of Integrals. *USSR Comput. Math. Math. Phys.* **1967**, 7, 86–112.

(39) Sobol, I. M. Uniformly Distributed Sequences with an Additional Uniform Property. *USSR Comput. Math. Math. Phys.* **1976**, 16, 236–242.

(40) Morokoff, W.; Caflisch, R. E. Quasi-Monte Carlo Integration. *J. Comput. Phys.* **1995**, 122, 218–230.

(41) Miller, W. H. Classical-Limit Quantum Mechanics and the Theory of Molecular Collisions. *Adv. Chem. Phys.* **1974**, 25, 69–177.

(42) Miller, W. H. The Classical S-Matrix in Molecular Collisions. *Adv. Chem. Phys.* **1975**, 30, 77–136.

(43) Beasley, J. D.; Springer, S. G. Algorithm AS 111: The Percentage Points of the Normal Distribution. *J. R. Stat. Soc. Ser. C, Appl. Stat.* **1977**, 26, 118–121.

(44) Kosloff, R. Time Dependent Quantum-Mechanical Methods for Molecular Dynamics. *J. Phys. Chem.* **1988**, 92, 2087–2100.

(45) Herman, M. F.; Arce, J. C. A Semiclassical Surface Hopping Formalism for Solvent-Induced Vibrational Relaxation. *Chem. Phys.* **1994**, 183, 335–350.

(46) Makri, N.; Miller, W. H. Coherent State Semiclassical Initial Value Representation for the Boltzmann Operator in Thermal Correlation Functions. *J. Chem. Phys.* **2002**, 116, 9207–9212.

(47) Shao, J.; Makri, N. Forward-Backward Semiclassical Dynamics Without Prefactors. *J. Phys. Chem. A* **1999**, 103, 7753–7756.

(48) Shao, J.; Makri, N. Forward-Backward Semiclassical Dynamics with Linear Scaling. *J. Phys. Chem. A* **1999**, 103, 9479–9486.

(49) Thompson, K.; Makri, N. Rigorous Forward-Backward Semiclassical Formulation of Many-Body Dynamics. *Phys. Rev. E* **1999**, 59, R4729–R4732.

(50) Shao, J.; Makri, N. Forward-Backward Semiclassical Dynamics in the Interaction Representation. *J. Chem. Phys.* **2000**, 113, 3681–3685.

(51) Wright, N. J.; Makri, N. Forward-Backward Semiclassical Dynamics for Condensed Phase Time Correlation Functions. *J. Chem. Phys.* **2003**, 119, 1634–1642.

(52) Liu, J.; Nakayama, A.; Makri, N. Long-Time Behaviour of Quantized Distributions in Forward-Backward Semiclassical Dynamics. *Mol. Phys.* **2006**, 104, 1267–1274.

(53) Lui, J.; Makri, N. Symmetries and Detailed Balance in Forward-Backward Semiclassical Dynamics. *Chem. Phys.* **2006**, 322, 23–29.

(54) Chen, J.; Makri, N. Time Correlation Functions via Forward-Backward Quantum Dynamics Using Hamilton's Law of Varying Action. *J. Chem. Phys.* **2009**, 131, No. 124107.

(55) Sun, X.; Miller, W. H. Forward-Backward Initial Value Representation of Semiclassical Time Correlation Functions. *J. Chem. Phys.* **1999**, 110, 6635–6644.

(56) Skinner, E.; Miller, W. H. Application of the Forward-Backward Initial Value Representation to Molecular Energy Transfer. *J. Chem. Phys.* **1999**, 111, 10787–10793.

(57) Thoss, M.; Wang, H.; Miller, W. H. Generalized Forward-Backward Initial Value Representation for the Calculation of Correlation Functions in Complex Systems. *J. Chem. Phys.* **2001**, 114, 9220–9235.

(58) Wang, H.; Thoss, M.; Sorge, K. L.; Gelabert, R.; Gimenez, X.; Miller, W. H. Semiclassical Description of Quantum Coherence Effects and Their Quenching: a Forward-Backward Initial Value Representation Study. *J. Chem. Phys.* **2001**, 114, 2562–2571.

(59) Gelabert, R.; Gimenez, X.; Thoss, M.; Wang, H.; Miller, W. H. Semiclassical Description of Diffraction and Its Quenching by the Forward-Backward Version of the Initial Value Representation. *J. Chem. Phys.* **2001**, 114, 2572–2579.

(60) Miller, W. H. Semiclassical Initial Value Representation: A Potentially Practical Way for Adding Quantum Effects to Classical Molecular Dynamics Simulations. *J. Phys. Chem.* **2001**, 105, 2942–2955.